for TEM analyses. Bright-field images of such cross sections were obtained with a Model CM-200T transmission electron microscope (Philips Electron Instruments). The scanning electron microscope and transmission electron microscope were both equipped with a Si/Li energy-dispersive X-ray detector (Edax International, Mahwah, NJ) for chemical analyses.

Received: November 19, 2001
Final version: January 2, 2002

[1] M. Madou, *Fundamentals of Microfabrication*, CRC Press, New York **1997**.
[2] C. S. Foong, K. L. Wood, I. Busch-Vishniac, in *Micromechanical Systems (MEMS) 1993* (Eds: A. P. Pisano, J. Jara-Almonte, W. Trimmer), ASME, New York **1993**, pp. 49–63.
[3] S. Britland, E. Perez-Arnaud, P. Clark, B. McGinn, P. Connolly, G. Moores, *Biotechnol. Prog.* **1992**, *8*, 155.
[4] T. A. Desai, D. Hansford, M. Ferrari, *J. Membr. Sci.* **1999**, *159*, 221.
[5] C. van Rijn, M. van der Wekken, W. Nijdam, M. Elsenspoek, *IEEE J. Microelectromech. Syst.* **1997**, *6*, 48.
[6] A. H. Epstein, S. D. Senturia, *Science* **1997**, *276*, 1211.
[7] A. M. Flynn, L. S. Tavrow, S. F. Bart, R. A. Brooks, D. J. Ehrlich, K. R. Udayakumar, L. E. Cross, *IEEE J. Microelectromech. Syst.* **1992**, *1*, 44.
[8] S. Mann, G. A. Ozin, *Nature* **1996**, *382*, 313.
[9] *Webster's Third New International Dictionary* (Ed: P. B. Gove), Merriam-Webster, Springfield, MA **1993**.
[10] H. Tappan, *The Paleobiology of Plant Protists*, W. H. Freeman, San Francisco, CA **1980**.
[11] F. E. Round, R. M. Crawford, D. G. Mann, *The Diatoms: Biology & Morphology of the Genera*, Cambridge University Press, Cambridge **1990**.
[12] J. C. Lewin, R. R. L. Guillard, *Annu. Rev. Microbiol.* **1963**, *17*, 373.
[13] S. A. Crawford, M. J. Higgins, P. Mulvaney, R. Wetherbee, *J. Phycol.* **2001**, *37*, 543.
[14] J. Parkinson, R. Gordon, *Trends Biotechnol.* **1999**, *17*, 190.
[15] M. W. Anderson, S. M. Holmes, N. Hanif, C. S. Cundy, *Angew. Chem. Int. Ed.* **2000**, *39*, 2707.
[16] R. W. Eppley, in *The Biology of Diatoms* (Ed: D. Werner), University of California Press, Berkeley, CA **1977**, pp. 24–64.
[17] U. Anderegg, S. Vorberg, K. Hermann, U. F. Haustein, *Eur. J. Dermatol.* **1997**, *7*, 27.
[18] M. C. Breslin, J. Ringnalda, L. Xu, M. Fuller, J. Seeger, G. S. Daehn, T. Otani, H. L. Fraser, *Mater. Sci. Eng. A* **1995**, *A195*, 113.
[19] W. G. Fahrenholtz, K. G. Ewsuk, D. T. Ellerby, R. E. Loehman, *J. Am. Ceram. Soc.* **1996**, *79*, 2497.
[20] F. Wagner, D. E. Garcia, A. Krupp, N. Claussen, *J. Eur. Ceram. Soc.* **1999**, *19*, 2449.
[21] P. Kumar, K. H. Sandhage, *J. Mater. Sci.* **1999**, *34*, 5757.
[22] K. A. Rogers, P. Kumar, R. Citak, K. H. Sandhage, *J. Am. Ceram. Soc.* **1999**, *82*, 757.
[23] R. Geffken, E. Miller, *Trans. AIME* **1968**, *242*, 2323.
[24] I. Barin, *Thermochemical Data of Pure Substances*, VCH, Weinheim, Germany **1989**.
[25] *Powder Diffraction File*, Cards No. 78–0430 for MgO, 35-0821 for Mg, 35-0773 for Mg_2Si, 45-1207 for Fe_3Si, International Center on Diffraction Data, Newtown Square, PA.
[26] O. Kubaschewski, *Iron—Binary Phase Diagrams*, Springer, New York **1982**.
[27] J. S. Lindberg, M. M. Zobitz, J. R. Poindexter, C. Y. C. Pak, *J. Am. Coll. Nutr.* **1990**, *9*, 48.
[28] D. N. Tallman, J. E. Pahlman, *Information Circular No. 9138*, US Bureau of Mines, Minneapolis, MN **1987**.
[29] T. Klicpera, M. Zdrazil, *Appl. Catal. A* **2001**, *216*, 41.
[30] *Handbook of Chemistry and Physics*, 55th ed., CRC Press, New York **1975**.
[31] A.-M. M. Schmid, R. K. Eberwein, M. Hesse, *Protoplasma* **1996**, *193*, 144.

Efficient Electroluminescent Devices Based on a Chelated Osmium(II) Complex**

By *Stefan Bernhard*, *Xicun Gao*, *George G. Malliaras*,* and *Héctor D. Abruña*

Advances in organic light-emitting diodes[1] have triggered intensive research effort towards the development of efficient solid-state electroluminescent materials.[2] Among the many different classes of materials currently under investigation, transition metal complexes (and especially 1,2-diimine complexes of Ru) have emerged as some of the most promising ones.[3–19] Early studies have shown the mechanism of operation of devices based on Ru complexes, which were either as discrete molecules or in polymeric form, to be dominated by the large amount of ionic charge. The mechanism of electroluminescence in these devices is in a way similar to electrogenerated chemiluminescence observed in solutions of these complexes.[20] The high efficiencies (as high as 24 %) achieved in solution[21] generated hope for high-performance solid-state devices. The first Ru-based solid-state devices had efficiencies that were fairly low, typically below 0.1 %.[3–7] Recently, however, Handy et al.[8,12] showed that efficiencies of the order of 1 % can be achieved in single layer devices made from $[Ru(bpy)_3]^{2+}(PF_6^-)_2$, where bpy is 2,2′-bipyridine. These devices achieved a brightness of 1000 cd m^{-2} at just 5 V, which is not too far from that of state-of-the-art organic light-emitting diodes. Additional progress by the MIT group has resulted in Ru-based devices with efficiencies up to 3 %.[22]

Transition metal complexes combine a variety of advantages. As demonstrated by the work on Ru complexes, efficient devices can be fabricated by using a single layer of active material that is processed by spin coating. These materials can be synthesized and purified with relative ease (compared to polymeric electroluminescent materials). Systematic electrochemical and spectroscopic studies in the past established a fairly detailed picture of their electronic structure, which can potentially lead to rapid progress in device performance. Finally, as we show here, efficient devices can be fabricated using air stable electrodes. One disadvantage of these complexes is their relatively long turn-on time, which is associated with the low mobility of the counter ions. It should be noted,

[*] Prof. G. G. Malliaras, Dr. X. Gao
Materials Science and Engineering, Cornell University
Ithaca, NY 14853 (USA)
E-mail: george@ccmr.cornell.edu
Dr. S. Bernhard, Prof. H. D. Abruña
Chemistry and Chemical Biology, Cornell University
Ithaca, NY 14853 (USA)

[**] Thanks are due to Yulong Shen, Jeff Mason, and Jennifer Ruglovsky for assistance with some of the experiments, and to J. Campbell Scott (IBM Almaden) for making available the CIE coordinates calculation software. This work was supported by the National Science Foundation (Career Award DMR-0094047) and by the Cornell Center for Materials Research (CCMR), a Materials Research Science and Engineering Center of the National Science Foundation (DMR-9632275). S.B. acknowledges a Fellowship for Advanced Researchers from the Swiss National Science Foundation (Grant 8220-053387).

  0935-9648/02/0603-0433 $ 17.50+.50/0

ADVANCED MATERIALS

though, that considerable progress has been achieved recently in reducing this turn-on time.[12,19,22]

In this communication, we report the fabrication and characterization of efficient, solid-state electroluminescent devices from the Os complex $[Os(bpy)_2L)]^{2+}(PF_6^-)_2$, where L is *cis*-1,2-bis(diphenylphosphino)ethylene (structure shown in the inset of Fig. 1). This complex, unlike $[Os(bpy)_3]^{2+}$, shows very intense room-temperature luminescence with an emission quantum yield three orders of magnitude greater than that of $[Os(bpy)_3]^{2+}$. The greater emission quantum yield can

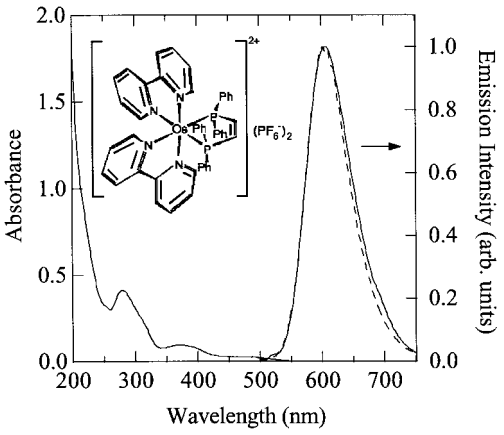

Fig. 1. UV-vis absorption and photoluminescence spectra of $[Os(bpy)_2L)]^{2+}(PF_6^-)_2$ in acetonitrile solution (0.01 mM) at room temperature. The dashed line is the electroluminescence spectrum from the ITO/$[Os(bpy)_2L)]^{2+}(PF_6^-)_2$/Au devices. The inset shows the chemical structure of $[Os(bpy)_2L)]^{2+}(PF_6^-)_2$.

be correlated with the strong π-backbonding ability of the phosphine ligand through the energy gap theorem. In fact, the emission quantum yield is comparable to that of $[Ru(bpy)_3]^{2+}(PF_6^-)_2$, but the phosphine ligands in $[Os(bpy)_2L)]^{2+}(PF_6^-)_2$ lead to a higher photo-stability compared to the aforementioned Ru^{II} complex.[23,24] Devices were fabricated by spin coating $[Os(bpy)_2L)]^{2+}(PF_6^-)_2$ on indium tin oxide (ITO) covered glass slides, using evaporated Au counter electrodes. Upon the application of a small bias voltage the devices emit red–orange light with an efficiency of the order of 1 %. Their brightness exceeds 6000 cd m^{-2} at 6 V and 330 cd m^{-2} at just 3 V, making osmium complexes a promising new class of solid-state emitters.

The synthesis, purification, and electrochemical properties of $[Os(bpy)_2L)]^{2+}$ have been reported in the past.[25,26] It undergoes reversible oxidation and reduction at potentials of E(ox) = +1.38 V and E(red) = –1.23 V vs. SSCE (sodium saturated calomel electrode), respectively. The lowest unoccupied molecular orbital (LUMO) is the π* orbital of the ligand and the highest occupied molecular orbitals (HOMO) are the t_{2g} orbitals of Os. Electrogenerated chemiluminescence (ECL) was observed in an electrochemical cell when the voltage applied to a Pt electrode was pulsed between E(ox) – E(red) = 2.61 V. The ECL spectrum was found to be identical to the solution photoluminescence spectrum (the latter is shown in Fig. 1), indicating that both spectra arise from the $\pi^* \rightarrow t_{2g}$ transition.

The solid-state devices were also found to operate at a low voltage. In Figure 2, the temporal evolution of the current and radiance (Fig. 2a) and the external quantum efficiency (Fig. 2b) are shown for various values of applied voltage. Each set of current and radiance curves was measured on a

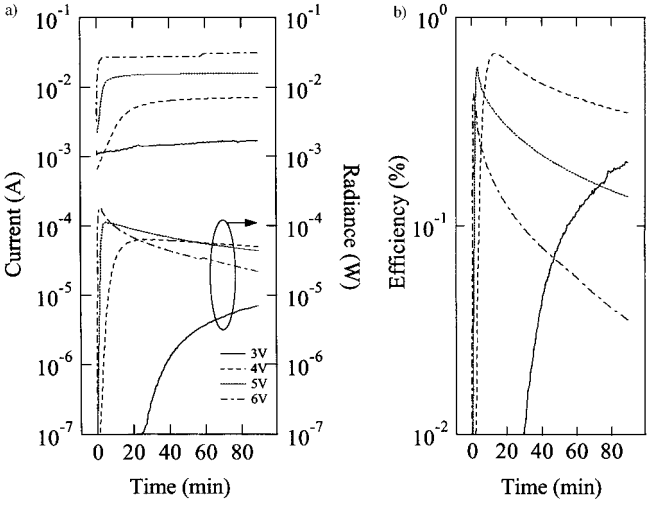

Fig. 2. Temporal evolution of the current and radiance (a), and external quantum efficiency (b) of ITO/$[Os(bpy)_2L)]^{2+}(PF_6^-)_2$/Au devices at various voltages. The thickness of the active layer was 105 nm.

fresh device in order to avoid artifacts due to device aging. Upon application of a voltage, the current increases to a steady-state value. The rise time decreases with applied voltage. At 3 V, the current continues to increase even 90 min after the voltage is turned on, while at 6 V the current saturates within three minutes. The radiance initially follows the current, but then decays at a rate that increases with voltage. The electroluminescence spectrum, shown in Figure 1, is virtually identical to the solution photoluminescence spectrum indicating that the $\pi^* \rightarrow t_{2g}$ transition is responsible for emission. The CIE coordinates were calculated to be x = 0.588 and y = 0.406, and are adequate for applications in monochrome displays. In order however for osmium complexes to be considered as red emitters in color displays, color tuning is required to produce compounds with spectra that are more shifted towards the red. A peak brightness of 6035 cd m^{-2} was observed at 6 V.

These characteristics are similar to those observed by Handy et al. in $[Ru(bpy)_3]^{2+}(PF_6^-)_2$ devices[12] and can be understood on the basis of the models developed by deMello et al.[27] and Pichot et al.[28] Upon application of a bias, the PF_6^- counter ions drift towards the anode (ITO), where they accumulate and cause a lowering of the barrier for hole injection. Holes are injected in the HOMO of $[Os(bpy)_2L)]^{2+}$, which corresponds to the removal of an electron from the t_{2g} orbital of Os and the production of $[Os(bpy)_2L)]^{3+}$. At the same time, the presence of uncompensated $[Os(bpy)_2L)]^{2+}$ ions in the neighborhood of the cathode enhances electron injection, which takes place in the π* orbital of the ligand and results in the formation of $[Os(bpy)_2L)]^{+}$. As the PF_6^- ions accumulate

  0935-9648/02/0603-0434 $ 17.50+.50/0

at the anode, hole and electron injection is enhanced, giving rise to the increase in current observed in Figure 2. A steady state is reached when the PF_6^- ions attain their equilibrium distribution near the anode, dictated by the applied bias and the coulombic interactions with the ionic and electronic charge in the device. It is believed that in steady-state situations, the applied bias is dropped at the contacts and holes and electrons move by diffusion only.[27,28] Light emission results from the electron transfer recombination of $[Os(bpy)_2L)]^{3+}$ and $[Os(bpy)_2L)]^{+}$ to produce $[Os(bpy)_2L)]^{2+*}$. A higher applied voltage speeds up the accumulation of the PF_6^- ions at the anode, giving rise to a faster device turn-on (Fig. 2).

The external quantum efficiency is shown in Figure 2 to follow the temporal evolution of the radiance. The lower the applied voltage, the higher the efficiency (the device reaches the highest efficiency at 3 V—not shown in this plot). The efficiency depends on the thickness of the $[Os(bpy)_2\ L)]^{2+}(PF_6^-)_2$ layer. As shown in the inset of Figure 3, it rises from 0.14 % to 1.1 % when the thickness is increased from 55 to 180 nm. Atomic force microscopy has shown the surface of these films

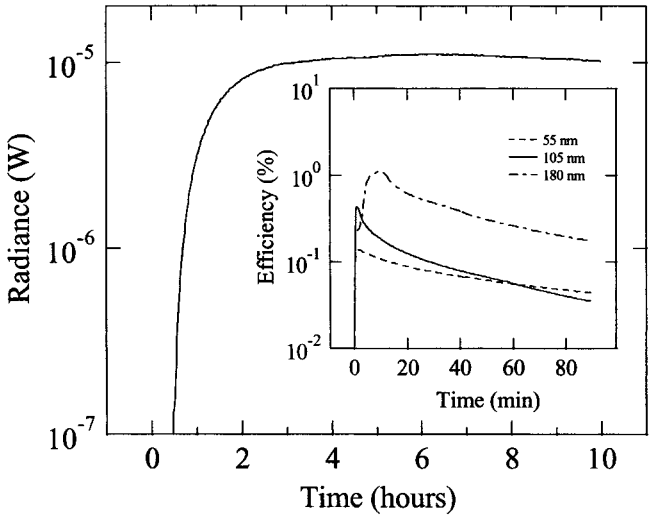

Fig. 3. Temporal evolution of the radiance of an ITO/$[Os(bpy)_2L)]^{2+}(PF_6^-)_2$/Au device with an active layer of 105 nm, at 3 V. Inset: Temporal evolution of the efficiency of devices with various thicknesses of the active layer, at 6 V.

to be smooth (the RMS roughness over an area of 25 μm^2 was smaller than one nanometer) and free of pinholes. The increase of efficiency with thickness is probably due to a reduction in the fraction of excitons that diffuse to (and are quenched at) the metal electrodes. As expected, the device with the thickest layer takes the longest time to turn on.

The origin of the degradation observed in the device efficiency is not fully understood at this moment. The fact that the current remains fairly constant while the radiance decays indicates that degradation is associated with a reduction in the yield of fluorescence, which takes place without affecting the transport properties of the film. The degradation was found to be permanent. The radiance of devices that were switched off, left to rest for a few hours and then switched back on again was only as high as that at the end of the first run. However, the degradation is dramatically slowed down at low voltages, implying that it is current induced. As shown in Figure 3, the device efficiency remains fairly constant over a period of 10 h, at a brightness of 335 cd m^{-2}.

In conclusion, chelated osmium complexes are promising new materials for solid-state electroluminescence. Efficient devices with air-stable electrodes were fabricated from $[Os(bpy)_2L)]^{2+}(PF_6^-)_2$. They exhibited red–orange emission with a peak radiance that exceeded 6000 cd m^{-2} at only 6 V. External quantum efficiencies that were of the order of 1 % were achieved. A characteristic turn-on time (which was less than 3 min at 6 V) indicated the importance of ionic space charge effects in the mechanism of device operation.

Experimental

The UV-vis absorption spectrum was recorded using a Hewlett-Packard 8453 diode-array spectrometer. The fluorescence spectrum was obtained using a SPEX 1681 Minimate-2 spectrofluorimeter. The excitation wavelength for the emission measurement was 450 nm. The spectrum was acquired normal to the incident beam. The solution spectrum was measured in acetonitrile (Mallinckrodt, HPLC grade) at a concentration of 0.01 mM. For the fabrication of the light-emitting devices, films were spin coated from an acetonitrile solution onto glass substrates covered with pre-patterned ITO (Thin Film Devices, Anaheim, CA). The ITO substrates were cleaned just before the deposition of the organic layer by a de-ionized water bath, followed by a UV/ozone treatment. The films were dried for 12 h at 100 °C under vacuum and were introduced in a dry nitrogen glove box for further processing and characterization. 200 Å thick Au cathodes were deposited through a shadow mask that defined six devices per substrate with a 3 mm^2 active area each. The deposition was carried out in an intermittent way in order to minimize heating of the organic film [27]. The electrical characteristics of the devices were measured with a Keithley 236 source-measure unit (with the ITO electrode wired as the anode) and the radiance with a calibrated UDT S370 optometer, coupled to an integrating sphere. The electroluminescence spectra were measured with a calibrated S2000 Ocean Optics fiber spectrometer. The emission was found to be uniform throughout the area of each device.

Received: October 29, 2001
Final version: January 10, 2002

[1] J. C. Scott, G. G. Malliaras, in *Conjugated Polymers* (Eds: G. Hadziioannou, P. F. van Hutten), WILEY-VCH **1999**, Ch. 13.
[2] See for example: N. R. Armstrong, R. M. Wightman, E. M. Gross, *Annu. Rev. Phys. Chem.* **2001**, *52*, 391.
[3] J.-K. Lee, D. S. Yoo, E. S. Handy, M. F. Rubner, *Appl. Phys. Lett.* **1996**, *69*, 1686.
[4] K. M. Maness, R. H. Terrill, T. J. Meyer, R. W. Murray, R. M. Wightman, *J. Am. Chem. Soc.* **1996**, *118*, 10 609.
[5] J.-K. Lee, D. Yoo, M. F. Rubner, *Chem. Mater.* **1997**, *9*, 1710.
[6] D. Yoo, A. Wu, J. Lee, M. F. Rubner, *Synth. Met.* **1997**, *85*, 1425.
[7] K. M. Maness, H. Masui, R. M. Wightman, R. W. Murray, *J. Am. Chem. Soc.* **1997**, *119*, 3987.
[8] E. S. Handy, E. D. Abbas, A. J. Pal, M. F. Rubner, *Proc. SPIE-Int. Soc. Opt. Eng.* **1998**, *3476*, 62.
[9] C. M. Elliot, F. Pichot, C. J. Bloom, L. S. Rider, *J. Am. Chem. Soc.* **1998**, *120*, 6781.
[10] A. Wu, J. Lee, M. F. Rubner, *Thin Solid Films* **1998**, *327–329*, 663.
[11] H. Lyons, E. D. Abbas, J.-K. Lee, M. F. Rubner, *J. Am. Chem. Soc.* **1998**, *120*, 12 100.
[12] E. S. Handy, A. J. Pal, M. F. Rubner, *J. Am. Chem. Soc.* **1999**, *121*, 3525.
[13] A. Wu, D. Yoo, J.-K. Lee, M. F. Rubner, *J. Am. Chem. Soc.* **1999**, *121*, 4883.
[14] M. M. Collinson, J. Taussig, S. A. Martin, *Chem. Mater.* **1999**, *11*, 2594.
[15] M. M. Collinson, S. A. Martin, *Chem. Commun.* **1999**, *899–900*, 899.
[16] W. Y. Ng, X. Gong, W. K. Chan, *Chem. Mater.* **1999**, *11*, 1165.
[17] W. K. Chan, P. K. Ng, X. Gong, S. Hou, *J. Mater. Chem.* **1999**, *9*, 2103.
[18] H. Rudmann, L. Kaplan, H. Sevian, M. F. Rubner, *Polym. Mater. Sci. Eng.* **2000**, *83*, 235.

  0935-9648/02/0603-0435 $ 17.50+.50/0

ADVANCED MATERIALS

[19] F. G. Gao, A. J. Bard, *J. Am. Chem. Soc*. **2000**, *122*, 7426.
[20] N. E. Tokel, A. J. Bard, *J. Am. Chem. Soc*. **1972**, *94*, 2862.
[21] P. McCord, A. J. Bard, *J. Electroanal. Chem.* **1991**, *318*, 91.
[22] H. Rudmann, M. F. Rubner, *J. Appl. Phys.* **2001**, *90*, 4338.
[23] H. D. Abruña, *J. Electroanal. Chem*. **1984**, *175*, 321.
[24] E. M. Kober, B. P. Sullivan, W. J. Dressick, J. V. Caspar, T. J. Meyer, *J. Am. Chem. Soc.* **1980**, *102*, 7383.
[25] J. V. Caspar, E. M. Kober, B. P. Sullivan, T. J. Meyer, *J. Am. Chem. Soc.* **1982**, *104*, 630.
[26] H. D. Abruña, *J. Electrochem. Soc*. **1985**, *132*, 842.
[27] J. C. deMello, N. Tessler, S. C. Graham, R. H. Friend, *Phys. Rev. B* **1998**, *52*, 12 951.
[28] F. Pichot, C. J. Bloom, L. S. Rider, C. M. Elliott, *J. Phys. Chem. B* **1998**, *102*, 3523.
[29] A. Ioannidis, J. S. Facci, M. A. Abkowitz, *J. Appl. Phys.* **1998**, *84*, 1439.

Oriented Crystalline Films of Tris(8-hydroxyquinoline) Aluminum(III): Growth of the Alpha Polymorph onto an Ultra-Oriented Poly(tetrafluoroethylene) Substrate**

By *Jean-François Moulin*, *Martin Brinkmann*,* *Annette Thierry*, and *Jean-Claude Wittmann*

Tris(8-hydroxyquinoline) aluminum(III) (Alq) has been the center of considerable interest since the first report of high luminance organic light-emitting diodes (OLED) by Tang and co-workers.[1] Most of the studies devoted to this material focussed on device optimization leading to high luminescence, long term stability, and fast response times.[2,3] More fundamental aspects of Alq such as its polymorphism were only recently investigated.[4] Brinkmann and co-workers isolated two non-solvated polymorphs of Alq and determined the crystal structures by X-ray diffraction on powders and single-crystals.[4] It was found that optical properties such as photoluminescence and absorption are intimately correlated to the molecular packing of the polymorphs.

To the best of our knowledge, none of these crystal structures have so far been reported in thin films grown by high-vacuum sublimation. Nevertheless, oriented crystalline films of Alq may be well adapted for applications such as polarized light emission,[5] organic field-effect transistors (OFETs),[6] or organic solid-state injection lasers,[7] which require oriented crystalline films.

Epitaxy is a common method for orienting molecules. It is achieved on a variety of substrates both inorganic (mica, alkali halides, HOPG graphite, ...) and organic (benzoic acid, anthracene, potassium acid phthalates, ...).[8] Ultra-thin polytetrafluoroethylene (PTFE) films obtained by friction transfer onto smooth substrates, such as silicon, glass, and ITO, constitute a powerful alternative to the latter substrates.[9] Oriented PTFE films have several advantages related to both orienting properties and processibility. The nucleating and orienting ability of this substrate has been demonstrated for a large variety of polymers and small molecules. Besides, PTFE films are easy to prepare, chemically inert, thermally stable up to 300 °C, optically transparent (visible range), and of low cost.

Two major growth mechanisms have been invoked to account for oriented crystallization on PTFE, namely true epitaxy and graphoepitaxy. Epitaxy involves 1D or 2D lattice matching between substrate and overgrowth. In the case of graphoepitaxy, the orienting action of the substrate is enforced by mesoscopic features of the substrate, such as macrosteps (ledges), independently of the molecular structure of the substrate and can therefore also be observed on amorphous substrates.[10] 1D and 2D epitaxy were evidenced in the cases of isotactic poly(propylene)[11] and para-nitroaniline[12] respectively, whereas graphoepitaxy was proposed to explain the orientation of poly(diacetylenes).[13] The main difficulty in the identification of the orienting mechanism stems from the fact that both the mesoscale relief and the atomically flat areas of the PTFE film share the same symmetry and crystal structure. Nevertheless, a recent study of the early stage of growth in vacuum deposited titanyl phthalocyanine onto PTFE has proven that PTFE macrosteps play a key role in the heterogeneous nucleation of nanocrystallites.[14]

In this paper, we report for the first time the possibility to control both crystallinity and orientation in sublimed Alq thin films. In addition, we highlight the essential role of the molecular structure of PTFE on the oriented growth mechanism. The overall results illustrate the possibility to pattern the structure of an organic overlayer by appropriate electron-beam irradiation of the PTFE substrate.

It is known that crystallinity in sublimed thin films of conjugated molecules is significantly enhanced by increasing the substrate temperature (T_s) during deposition.[16] In Figure 1, we depict a sequence of transmission electron microscopy (TEM) images showing the evolution of the film morphology as a function of increasing T_s (50 °C ≤ T_s ≤ 100 °C). In this narrow T_s range, we can observe a drastic modification of the film morphology. As shown in Figure 1a, for T_s = 50 °C, Alq films exhibit a microstructured pattern with periodicity in the range 0.15–0.30 μm, which is similar to that observed for dewetting polymer films. The absence of reflections in the ED pattern points at the amorphous character of the films.

For T_s = 63 °C (Fig. 1b), a clear change in the film morphology is observed. The films consist of a dominant microstructured texture similar to that observed for T_s = 50 °C, which coexists with needle-shaped microcrystallites of mean size 1–2 μm. Similarly to titanyl phthalocyanine, we observe a preferential nucleation of Alq microcrystallites at PTFE macrosteps.[14] This observation highlights the heterogeneous nature of nucleation on PTFE. Moreover, the value of T_s at which crystallization is observed on PTFE lies much below the temperature of crystallization for amorphous bulk Alq for which a characteristic exotherm centered at T = 179 °C is evi-

[*] Dr. M. Brinkmann, Dr. J.-F. Moulin, Dr. A. Thierry, Dr. J.-C. Wittmann
Institut Charles Sadron, UPR 22 CNRS
6 rue Boussingault, F-67083 Strasbourg CEDEX (France)
E-mail: brinkman@ics.u-strasbg.fr

[**] This work was supported by EEC contract ERB FMRXCT 970106. C. Straupé and S. Zehnacker are acknowledged for technical support as well as B. Lotz and M. Schmutz for fruitful discussions.

  0935-9648/02/0603-0436 $ 17.50+.50/0